

Supporting Information

Heteroleptic Ir(III) Phosphors with Bis-Tridentate Chelating Architecture for High Efficiency OLEDs

Bihai Tong,^a Hsiao-Yun Ku,^a I-Jen Chen,^a Yun Chi,^{a,*} Hao-Che Kao,^b Chia-Chi Yeh,^b Chih-Hao Chang,^{b,*} Shih-Hung Liu,^c Gene-Hsiang Lee,^c and Pi-Tai Chou^{c,*}

^a Department of Chemistry, National Tsing Hua University, Hsinchu 30013, Taiwan

^b Department of Photonics Engineering, Yuan Ze University, Chungli 32003, Taiwan

^c Department of Chemistry and Instrumentation Center, National Taiwan University, Taipei 10617, Taiwan

Contents		Page
Detailed Synthesis and Characterizations		S3
Table S1	The calculated transfer character of the five lowest singlet and triplet optical transitions for complex 1	S7
Figure S1	Frontier molecular orbitals pertinent to the optical transitions for complex 1 .	S8
Table S2	The calculated transfer character of the five lowest singlet and triplet optical transitions for complex 2	S9
Figure S2	Frontier molecular orbitals pertinent to the optical transitions for complex 2 .	S10
Table S3	The calculated transfer character of the five lowest singlet and triplet optical transitions for complex 3	S11
Figure S3	Frontier molecular orbitals pertinent to the optical transitions for complex 3 .	S12
Table S4	The calculated transfer character of the five lowest singlet and triplet optical transitions for complex 4	S13
Figure S4	Frontier molecular orbitals pertinent to the optical transitions for complex 4 .	S14
Table S5	The calculated transfer character of the five lowest singlet and triplet optical transitions for complex 5	S15
Figure S5	Frontier molecular orbitals pertinent to the optical transitions for complex 5 .	S16
Table S6	The calculated transfer character of the five lowest singlet and triplet optical transitions for complex 6	S17
Figure S6	Frontier molecular orbitals pertinent to the optical transitions for complex 6 .	S18

Synthesis of 1,3-difluoro-4,6-di(4-*t*-butylpyridin-2-yl) benzene (L2).

The 100 mL round bottom flask was sequentially added a mixture of dimethoxyethane (50 mL), 1,3-(4,6-difluorophenyl)diboronic acid bis(pinacol) ester (1 g, 2.7 mmol), 4-(*tert*-butyl)-2-bromopyridine (1.29 g, 6 mmol), 2N Na₂CO₃ (15 mL) and Pd(PPh₃)₂Cl₂ (0.32 g, 0.27 mmol). The mixture was refluxed 48 h under nitrogen. The reaction mixture was cooled to room temperature, concentrated by evaporation, dissolved in ethyl acetate (EA) and neutralized with saturated aqueous Na₂CO₃ solution. The organic phase was washed with brine and dried over Na₂SO₄, the solvent was removed under vacuum to give a crude product. The solid was first purified using SiO₂ column chromatography eluting with a mixture of EA and hexane (1:3.5) to obtain the colorless liquid (520 mg, 50%).

Spectral data: ¹H NMR (400 MHz, d₆-acetone): δ 8.74 (t, *J* = 9.2 Hz, 1H), 8.64 (d, *J* = 5.2 Hz, 2H), 7.88 (s, 2 H), 7.43 (dd, *J* = 5.2, 2.0 Hz, 2H), 7.30 (t, *J* = 11.2 Hz, 1H), 1.38 (s, 18 H). ¹⁹F NMR (376 MHz, d₆-acetone): δ -113.42 (t, *J* = 10.2 Hz).

Synthesis of 1,3-(4-*t*-butylphenyl)diboronic acid bis(pinacol) ester.

A mixture of 1,3-dibromo-5-*t*-butylbenzene (2.9 g, 10 mmol), bis(pinacolato)diboron (5 g, 20 mmol), KOAc (4.9 g, 50 mmol) and Pd(dppf)Cl₂ (0.5 g, 0.7 mmol) in 1,4-dioxane (100 mL) was stirred at 100 °C for 12 h. The reaction mixture was then poured into water and extracted with EA. The organic extracts were washed with brine and dried with anhydrous Na₂SO₄. After removal of the solvent, the residue was purified by silica gel column chromatography (hexane, silica gel) to afford product as a white solid (2.4 g, 63%).

Spectral data: ¹H NMR (CDCl₃, 400 MHz): δ 8.09 (s, 1 H), 7.91 (s, 2H), 1.34 (s, 9H), 1.32 (s, 24H).

Synthesis of 1,3-di(pyridine-2-yl)-5-*tert*-butylbenzene (L3).

2-Bromopyridine (3.2 g, 20 mmol), 1,3-(4-*t*-butylphenyl)diboronic acid bis(pinacol) ester (3.9 g, 10 mmol), Na₂CO₃ (3 g, 30 mmol) and Pd(PPh₃)₄ (0.5g, 0.4

mmol) were dissolved in 30 mL of dimethoxyethane and H₂O (v/v = 1:1) and the mixture was refluxed with stirring for 24 h under N₂. After cooled to RT, the mixture was poured into water and extracted with EA. The organic extracts were washed with brine and dried with anhydrous Na₂SO₄. After removal of the solvent, the crude product was purified by silica gel column chromatography (EA/hexane, 1/5, v/v) to afford a colorless solid (2.3 g, 81%).

Spectral data: ¹H NMR (CDCl₃, 400 MHz): δ 8.70 (d, *J* = 5.6 Hz, 2 H), 8.35 (s, 1H), 8.12 (s, 2H), 7.81 (d, *J* = 6.0 Hz, 2H), 7.73 (t, *J* = 7.6 Hz, 2H), 7.19 ~ 7.22 (m, 2H), 1.44 (s, 9H).

Synthesis of 4-*t*-butyl-2,6-di(isoquinolin-1-yl) benzene (L4).

Synthesized using 1-chloroisoquinoline according to the previous method. Crude product was purified by column chromatography on silica gel using a 1:4 mixture of hexane and EA as eluent. White solid. Yield: 52%.

Spectral data: ¹H NMR (CDCl₃, 400 MHz): δ 8.60 (d, *J* = 6.0 Hz, 2H), 8.16 (d, *J* = 9.2 Hz, 2H), 7.85 (s, 2H), 7.82 (d, *J* = 8.0 Hz, 2H), 7.79 (t, *J* = 1.6 Hz, 1H), 7.60-7.64 (m, 4H), 7.49 (t, *J* = 7.2 Hz, 2H), 1.42 (s, 9H).

Synthesis of 1-(6-(4-trifluoromethylphenyl)pyridin-2-yl) ethanone.

The 100 mL round bottom flask was sequentially added a mixture of toluene and MeOH (v/v, 9:1, 50 mL), 1-(6-bromopyridin-2-yl) ethanone (900 mg, 4.5 mmol), 1,3-(4-trifluoromethylphenyl)diboronic acid bis(pinacol) ester (1.36 g, 4.95 mmol), 2N Na₂CO_{3(aq)} (11 mL, 22.5 mmol) and Pd(PPh₃)₄ (260 mg, 0.22 mmol). The mixture was refluxed for 24 h under nitrogen and then cooled to RT. The THF was evaporated and the residue was dissolved in excess of EA. The resulting mixture was filtered, and the filtrate washed with brine, dried over Na₂SO₄, and then concentrated. The solid was first purified using SiO₂ column chromatography eluting with a mixture of EA and hexane (1:6). Recrystallization from a mixed solution of CH₂Cl₂ and hexane gave a white solid (891 mg, 75%).

Spectral data: ^1H NMR (400 MHz, CDCl_3 , 294 K): δ 8.02 (d, $J = 6.4$, 2 H), 7.95 (d, $J = 7.6$ Hz, 1 H), 7.93 ~ 7.91 (m, 2 H), 7.75 (d, $J = 8.0$, 2 H), 2.81 (s, 3 H). ; ^{19}F NMR (376 MHz, CDCl_3): δ -62.59(s).

Synthesis of 1-(6-(4-(*t*-butylphenyl)pyridin-2-yl)ethanone.

Synthesized using 1,3-(4-*t*-butylphenyl)diboronic acid bis(pinacol) ester according to the previous method. Crude product was purified by column chromatography on silica gel using a mixture of hexane/ EA (5:1) as eluent. Yellow liquid. Yield: 98%.

Spectral data: ^1H NMR (400 MHz, CDCl_3): δ 8.02 (d, $J_{\text{HH}} = 8.4$ Hz, 2H), 7.94 ~ 7.83 (m, 3H), 7.52 (d, $J_{\text{HH}} = 8.4$ Hz, 2H), 2.8 (s, 3H), 1.36 (s, 9H).

Synthesis of 2-(3-(trifluoromethyl)-1H-pyrazol-5-yl)-6-(4-trifluoromethylphenyl)pyridine.

To a stirred suspension of NaOEt (335 mg, 4.90 mmol) in dry THF (50 mL) was slowly added 1-(6-(4-(trifluoromethyl)phenyl)pyridin-2-yl) ethanone (870 mg, 3.28 mmol) at 0 °C. The resultant solution was stirred for 1 h at room temperature. Ethyl trifluoroacetate (0.62 mL, 4.9 mmol) was added dropwise at 0 °C and the mixture was refluxed for 12 h. After then, the content was quenched with 2N HCl until pH 5-6 and extracted three times with EA. The combined organic phase was washed with brine, dried over Na_2SO_4 , and concentrated under vacuum to yield the crude 1,3-dione. To the crude 1,3-dione was added hydrazine monohydrate (1.6 mL, 32.8 mmol) in 50 mL of EtOH and refluxed for 1 day. The reaction mixture was cooled to room temperature, concentrated by evaporation, dissolved in EA and neutralized with saturated aqueous Na_2CO_3 solution. The organic phase was washed with brine and dried over Na_2SO_4 , the solvent was removed under vacuum to give a crude product. Finally, the crude product was purified by SiO_2 column chromatography and eluting with a mixture of EA and hexane (1:3). Recrystallization from a mixed solution of CH_2Cl_2 and hexane gave a white solid (0.84 g, 70%).

Spectral data: ^1H NMR (400 MHz, CDCl_3): δ 11.42 (br, 1 H), 8.12 (d, $J = 8.0$ Hz, 2 H), 7.90 (t, $J = 7.8$ Hz, 1 H), 7.75 (d, $J = 8.0$ Hz, 3 H), 7.61 (d, $J = 8.0$ Hz, 1 H), 6.99 (s, 1 H). ^{19}F NMR (376 MHz, CDCl_3): δ -62.35(s, 3 H), -62.69(s, 3 H).

Synthesis of 2-(3-(*t*-butyl)-1H-pyrazol-5-yl)-6-(4-trifluoromethylphenyl) pyridine.

It was synthesized using 1-(6-(4-*t*-butylphenyl)pyridin-2-yl)ethanone according to the previous method. Crude product was purified by column chromatography on silica gel using a mixture of hexane/ EA (5:1) as eluent. White solid. Yield: 56%.

Spectral data: ^1H NMR (400 MHz, CDCl_3): δ 7.95 (dd, $J_{\text{HH}} = 8.4, 2.0$ Hz, 2H), 7.83 (t, $J_{\text{HH}} = 8.0$ Hz 1H), 7.70 (d, $J_{\text{HH}} = 8.0$ Hz 1H), 7.54 (d, $J_{\text{HH}} = 2.0$ Hz, 1H), 7.53 ~ 7.51 (m, 2H), 6.96 (s, 1H), 1.37 (s, 9H). ^{19}F NMR (376 MHz, CDCl_3): δ -62.37 (s, 3 F).

Table S1. The calculated wavelengths, transition probabilities and charge transfer character of the five lowest singlet and triplet optical transitions for complex **1** in dichloromethane.

State	λ (nm)	f	Assignments	MLCT
T ₁	454.6	0	HOMO \rightarrow LUMO+1 (39%) HOMO \rightarrow LUMO (24%) HOMO-5 \rightarrow LUMO+1 (8%) HOMO \rightarrow LUMO+3 (7%)	20.16%
T ₂	445	0	HOMO \rightarrow LUMO (17%) HOMO-3 \rightarrow LUMO (16%) HOMO-1 \rightarrow LUMO+2 (14%) HOMO \rightarrow LUMO+1 (12%) HOMO-4 \rightarrow LUMO (9%) HOMO-2 \rightarrow LUMO (9%)	20.41%
T ₃	430.5	0	HOMO-1 \rightarrow LUMO (68%) HOMO-1 \rightarrow LUMO+1 (18%)	29.92%
T ₄	413.9	0	HOMO \rightarrow LUMO+3 (46%) HOMO-2 \rightarrow LUMO+3 (22%) HOMO \rightarrow LUMO+1 (14%) HOMO \rightarrow LUMO (5%)	22.01%
T ₅	412	0	HOMO-1 \rightarrow LUMO+2 (73%) HOMO \rightarrow LUMO (11%) HOMO \rightarrow LUMO+1 (7%)	27.22%
S ₁	389.8	0.0338	HOMO \rightarrow LUMO (47%) HOMO \rightarrow LUMO+1 (45%) HOMO \rightarrow LUMO+3 (6%)	28.56%
S ₂	387.5	0.0659	HOMO-1 \rightarrow LUMO (70%) HOMO \rightarrow LUMO+2 (25%)	30.89%
S ₃	379.8	0.0004	HOMO-1 \rightarrow LUMO+1 (78%) HOMO-1 \rightarrow LUMO (12%) HOMO \rightarrow LUMO+2 (8%)	32.10%
S ₄	376.5	0.0083	HOMO \rightarrow LUMO+1 (42%) HOMO \rightarrow LUMO (39%) HOMO-1 \rightarrow LUMO+2 (15%)	28.06%
S ₅	370.8	0.1474	HOMO \rightarrow LUMO+2 (62%) HOMO-1 \rightarrow LUMO+1 (17%) HOMO-1 \rightarrow LUMO (16%)	26.76%

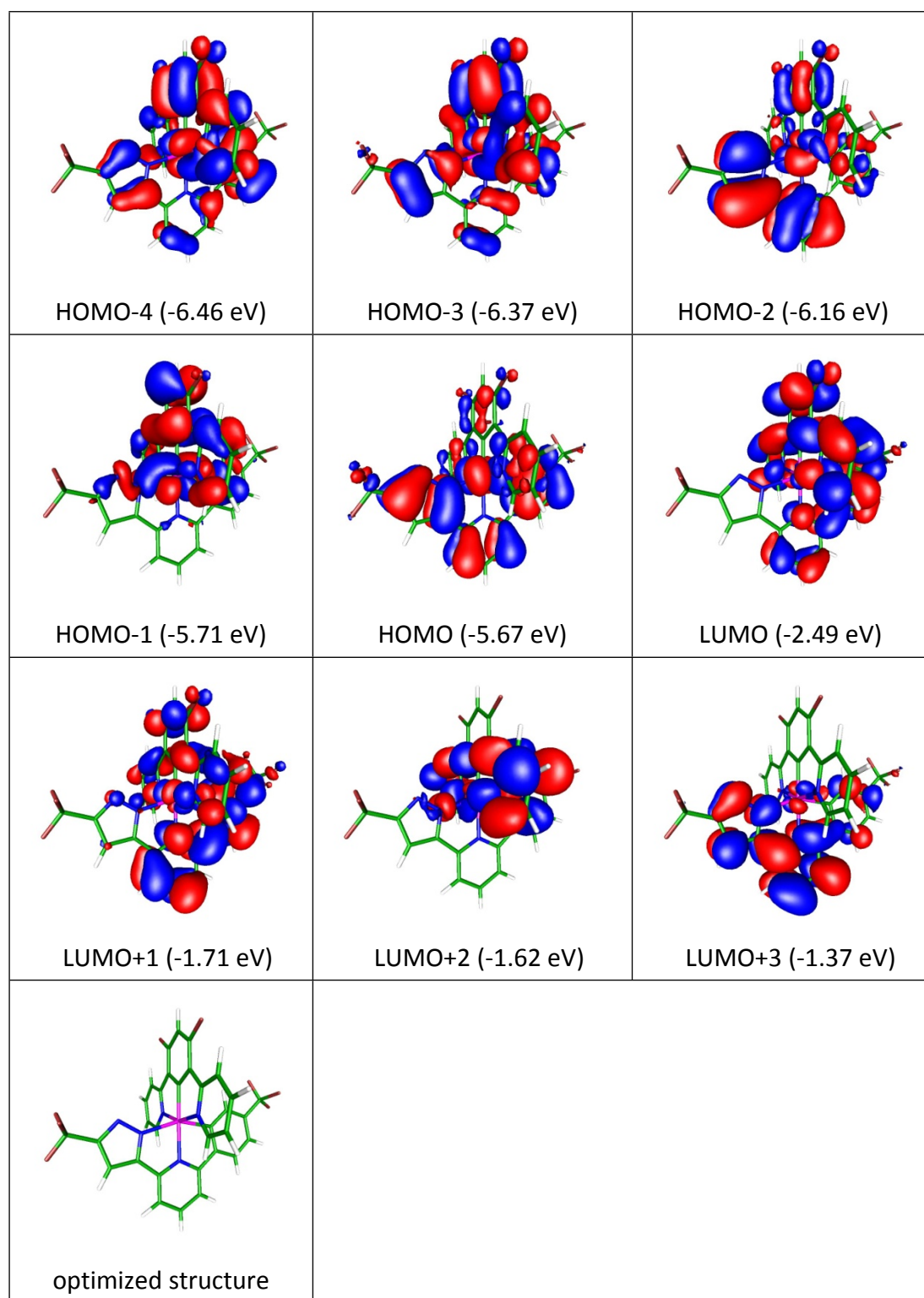


Figure S1. Frontier molecular orbitals pertinent to the optical transitions for complex **1**. For the clarity of viewing, the optimized structure with no involvement of frontier orbitals is shown at the last figure.

Table S2. The calculated wavelengths, transition probabilities and charge transfer character of the five lowest singlet and triplet optical transitions for complex **2** in dichloromethane.

State	λ (nm)	f	Assignments	MLCT
T ₁	456.1	0	HOMO → LUMO (56%) HOMO-5 → LUMO (10%) HOMO → LUMO+1 (8%) HOMO → LUMO+3 (6%)	21.81%
T ₂	436.6	0	HOMO → LUMO+1 (23%) HOMO-3 → LUMO+1 (19%) HOMO-1 → LUMO+2 (11%) HOMO-2 → LUMO+1 (8%) HOMO-4 → LUMO+1 (8%) HOMO-3 → LUMO (6%)	19.36%
T ₃	423.3	0	HOMO-1 → LUMO+1 (62%) HOMO-1 → LUMO (23%)	29.25%
T ₄	414.7	0	HOMO → LUMO+3 (45%) HOMO-2 → LUMO+3 (23%) HOMO → LUMO (14%)	21.74%
T ₅	403.9	0	HOMO-1 → LUMO+2 (73%) HOMO → LUMO+1 (12%)	25.86%
S ₁	392.3	0.0296	HOMO → LUMO (84%) HOMO → LUMO+1 (8%) HOMO → LUMO+3 (6%)	30.52%
S ₂	386.4	0.0219	HOMO-1 → LUMO (95%)	32.92%
S ₃	379.1	0.0828	HOMO-1 → LUMO+1 (78%) HOMO → LUMO+2 (19%)	31.88%
S ₄	369.1	0.0095	HOMO → LUMO+1 (74%) HOMO-1 → LUMO+2 (15%) HOMO → LUMO (7%)	29.57%
S ₅	363.7	0.1873	HOMO → LUMO+2 (73%) HOMO-1 → LUMO+1 (18%)	25.81%

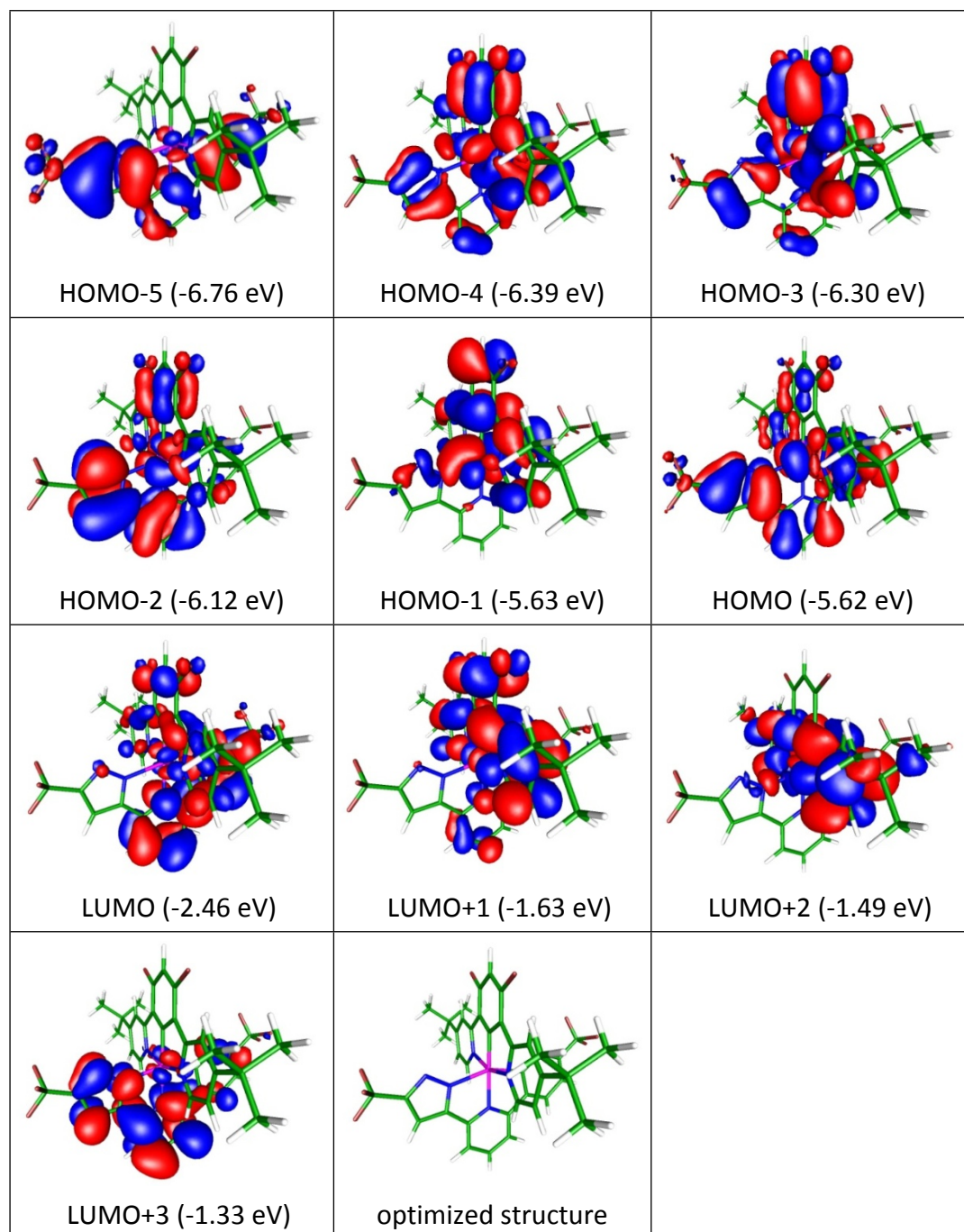


Figure S2. Frontier molecular orbitals pertinent to the optical transitions for complex **2**. For the clarity of viewing, the optimized structure with no involvement of frontier orbitals is shown at the last figure.

Table S3. The calculated wavelengths, transition probabilities and charge transfer character of the five lowest singlet and triplet optical transitions for complex **3** in dichloromethane.

State	λ (nm)	f	Assignments	MLCT
T ₁	483.7	0	HOMO → LUMO (83%) HOMO → LUMO+1 (10%)	29.21%
T ₂	461.4	0	HOMO → LUMO+2 (27%) HOMO-1 → LUMO (23%) HOMO-4 → LUMO (17%) HOMO-3 → LUMO (7%)	17.99%
T ₃	456	0	HOMO-1 → LUMO+1 (55%) HOMO-5 → LUMO+1 (9%) HOMO-1 → LUMO (6%) HOMO-1 → LUMO+3 (6%)	20.29%
T ₄	433.8	0	HOMO → LUMO+2 (61%) HOMO-1 → LUMO (18%)	22.05%
S ₁	415.9	0.1214	HOMO → LUMO (94%)	29.74%
T ₅	414.6	0	HOMO-1 → LUMO+3 (41%) HOMO-2 → LUMO+3 (19%) HOMO-1 → LUMO+1 (15%) HOMO → LUMO+1 (8%)	24.55%
S ₂	407.3	0.0269	HOMO → LUMO+1 (96%)	28.31%
S ₃	393.4	0.0328	HOMO-1 → LUMO (50%) HOMO-1 → LUMO+1 (36%) HOMO-1 → LUMO+3 (6%) HOMO → LUMO+2 (6%)	30.51%
S ₄	388.5	0.005	HOMO → LUMO+2 (62%) HOMO-1 → LUMO+1 (31%)	25.85%
S ₅	377.9	0.0331	HOMO-1 → LUMO (42%) HOMO → LUMO+2 (28%) HOMO-1 → LUMO+1 (24%)	28.28%

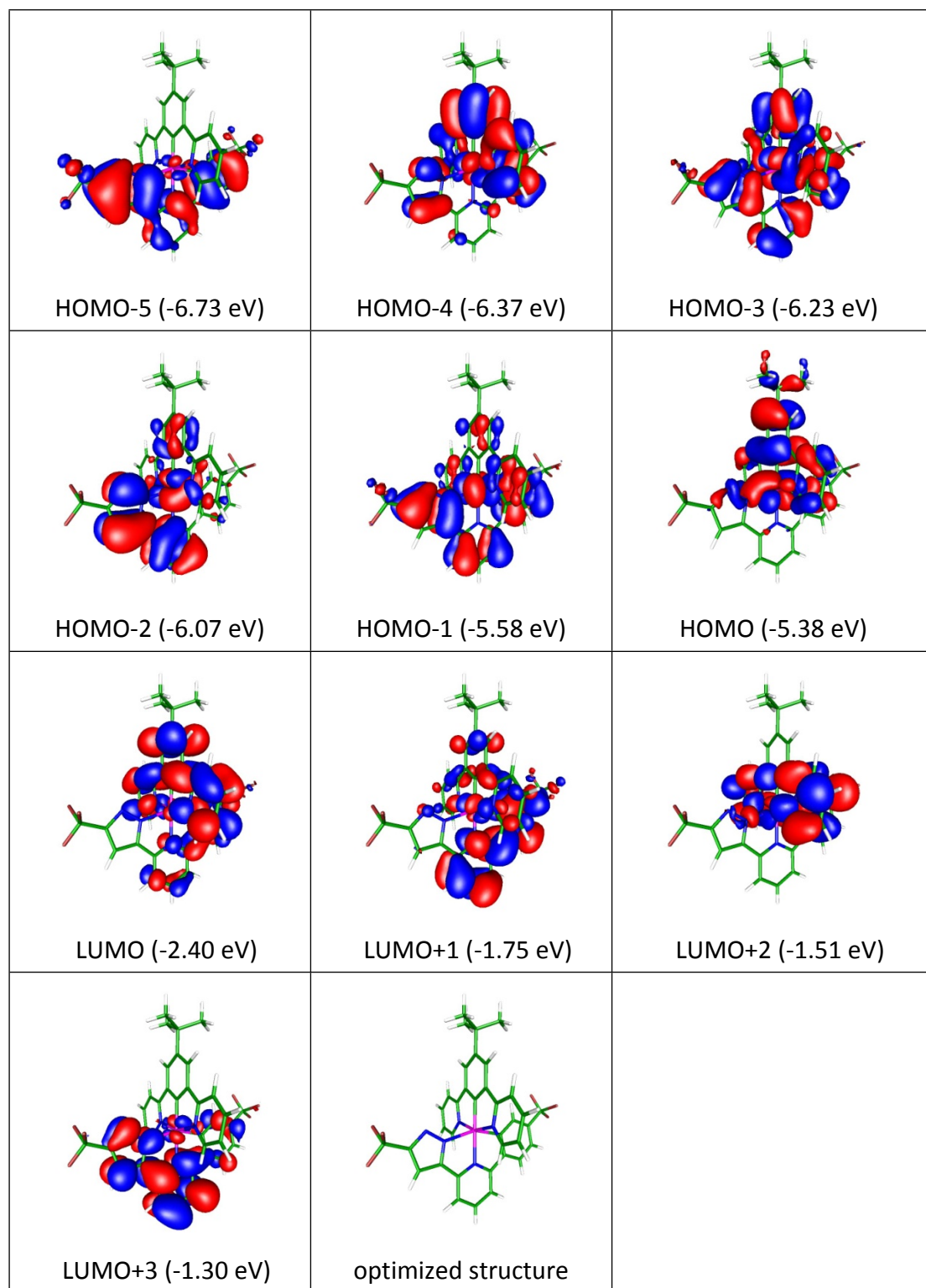


Figure S3. Frontier molecular orbitals pertinent to the optical transitions for complex **3**. For the clarity of viewing, the optimized structure with no involvement of frontier orbitals is shown at the last figure.

Table S4. The calculated wavelengths, transition probabilities and charge transfer character of the five lowest singlet and triplet optical transitions for complex **4** in dichloromethane.

State	λ (nm)	f	Assignments	MLCT
T ₁	490.8	0	HOMO \rightarrow LUMO (94%)	30.63%
T ₂	464.8	0	HOMO \rightarrow LUMO+1 (27%) HOMO-4 \rightarrow LUMO (27%) HOMO-1 \rightarrow LUMO (24%) HOMO-2 \rightarrow LUMO (6%)	15.09%
T ₃	446	0	HOMO-1 \rightarrow LUMO+2 (35%) HOMO-1 \rightarrow LUMO+3 (20%) HOMO-2 \rightarrow LUMO+3 (12%) HOMO-3 \rightarrow LUMO+2 (8%) HOMO-5 \rightarrow LUMO+2 (5%)	20.71%
T ₄	442.4	0	HOMO \rightarrow LUMO+1 (58%) HOMO-1 \rightarrow LUMO (22%)	22.61%
S ₁	421.8	0.1303	HOMO \rightarrow LUMO (91%) HOMO-1 \rightarrow LUMO+1 (7%)	31.38%
T ₅	415.6	0	HOMO-1 \rightarrow LUMO+1 (65%) HOMO-1 \rightarrow LUMO+2 (7%) HOMO-1 \rightarrow LUMO+3 (5%)	19.51%
S ₂	401.8	0.015	HOMO-1 \rightarrow LUMO (78%) HOMO \rightarrow LUMO+1 (19%)	28.38%
S ₃	387.5	0.0297	HOMO \rightarrow LUMO+1 (73%) HOMO-1 \rightarrow LUMO (17%)	25.29%
S ₄	386.3	0.0005	HOMO \rightarrow LUMO+2 (95%)	28.88%
S ₅	383.4	0.0734	HOMO-1 \rightarrow LUMO+1 (61%) HOMO-1 \rightarrow LUMO+2 (29%)	23.08%

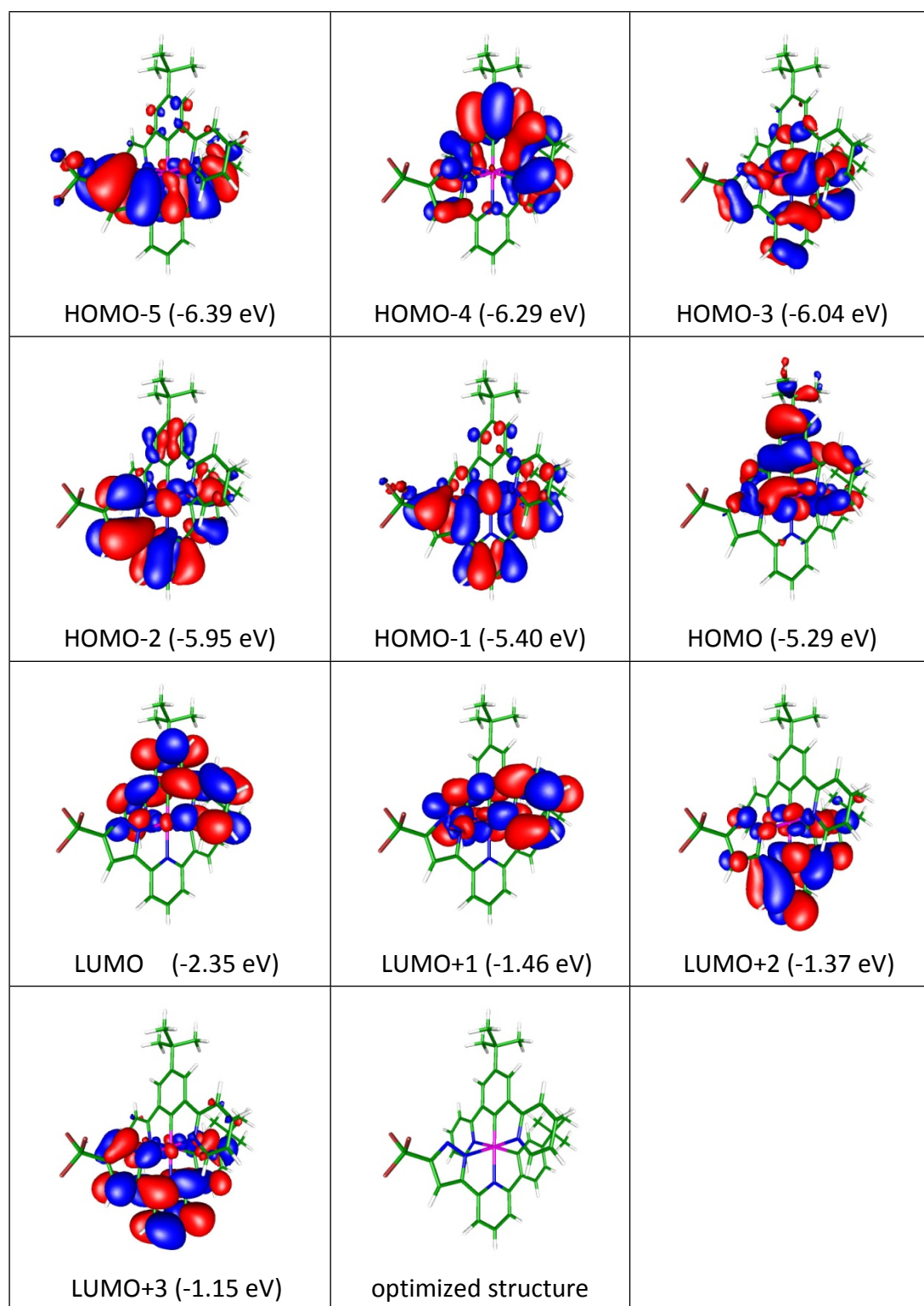


Figure S4. Frontier molecular orbitals pertinent to the optical transitions for complex **4**. For the clarity of viewing, the optimized structure with no involvement of frontier orbitals is shown at the last figure.

Table S5. The calculated wavelengths, transition probabilities and charge transfer character of the five lowest singlet and triplet optical transitions for complex **5** in dichloromethane.

State	λ (nm)	f	Assignments	MLCT
T ₁	567.3	0	HOMO → LUMO (30%) HOMO-1 → LUMO (27%) HOMO → LUMO+1 (10%) HOMO-2 → LUMO (8%) HOMO-3 → LUMO (7%) HOMO-5 → LUMO+1 (7%)	22.65%
T ₂	559.1	0	HOMO → LUMO (50%) HOMO-1 → LUMO (19%)	19.71%
T ₃	496.5	0	HOMO-1 → LUMO+1 (38%) HOMO-5 → LUMO (18%) HOMO → LUMO (15%) HOMO → LUMO+1 (10%) HOMO-2 → LUMO+1 (6%)	19.27%
T ₄	489.2	0	HOMO → LUMO+1 (69%) HOMO-1 → LUMO (15%) HOMO-1 → LUMO+1 (7%)	23.57%
S ₁	473.8	0.2674	HOMO → LUMO (96%)	26.35%
T ₅	458.9	0	HOMO-1 → LUMO+2 (58%) HOMO-6 → LUMO+2 (10%) HOMO-2 → LUMO+3 (5%)	18.04%
S ₂	444.9	0.0314	HOMO-1 → LUMO (84%) HOMO → LUMO+1 (13%)	29.63%
S ₃	427.3	0.0329	HOMO → LUMO+1 (79%) HOMO-1 → LUMO (11%) HOMO-1 → LUMO+1 (6%)	24.46%
S ₄	422	0.0602	HOMO-1 → LUMO+1 (88%) HOMO → LUMO+1 (6%)	26.51%
S ₅	405.3	0.0049	HOMO → LUMO+2 (97%)	25.43%

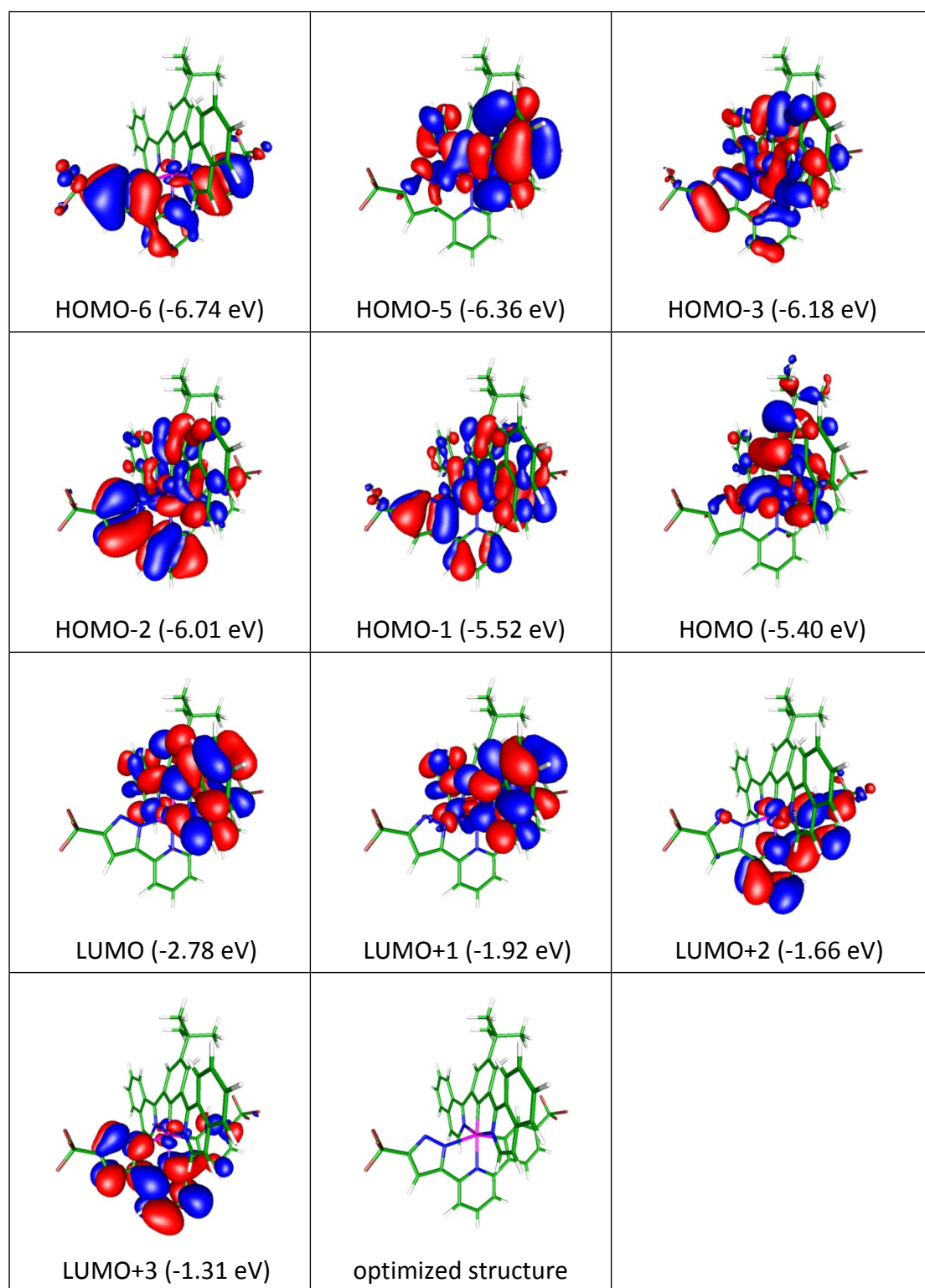


Figure S5. Frontier molecular orbitals pertinent to the optical transitions for complex **5**. For the clarity of viewing, the optimized structure with no involvement of frontier orbitals is shown at the last figure.

Table S6. The calculated wavelengths, transition probabilities and charge transfer character of the five lowest singlet and triplet optical transitions for complex **6** in dichloromethane.

State	λ (nm)	f	Assignments	MLCT
T ₁	574.8	0	HOMO → LUMO (44%) HOMO-1 → LUMO (17%) HOMO-2 → LUMO (9%) HOMO → LUMO+1 (8%) HOMO-4 → LUMO (6%) HOMO-5 → LUMO+1 (6%)	20.90%
T ₂	566.6	0	HOMO → LUMO (37%) HOMO-1 → LUMO (32%) HOMO-2 → LUMO (6%)	19.85%
T ₃	506.3	0	HOMO-1 → LUMO+1 (31%) HOMO → LUMO+1 (23%) HOMO-5 → LUMO (14%) HOMO → LUMO (13%) HOMO-2 → LUMO+1 (7%)	19.18%
T ₄	499.9	0	HOMO → LUMO+1 (55%) HOMO-1 → LUMO+1 (20%) HOMO-1 → LUMO (14%)	23.36%
S ₁	482.5	0.2437	HOMO → LUMO (91%)	26.04%
S ₂	465.1	0.0294	HOMO-1 → LUMO (90%) HOMO → LUMO+1 (5%)	38.88%
T ₅	451.3	0	HOMO-1 → LUMO+2 (35%) HOMO-1 → LUMO+3 (15%) HOMO-2 → LUMO+3 (8%) HOMO-1 → LUMO (7%)	16.87%
S ₃	439	0.0701	HOMO-1 → LUMO+1 (71%) HOMO → LUMO+1 (22%)	24.09%
S ₄	432.1	0.0339	HOMO → LUMO+1 (70%) HOMO-1 → LUMO+1 (22%) HOMO-1 → LUMO (5%)	25.12%
S ₅	394.5	0.0006	HOMO-3 → LUMO (50%) HOMO-2 → LUMO (41%) HOMO-1 → LUMO+2 (6%)	28.70%

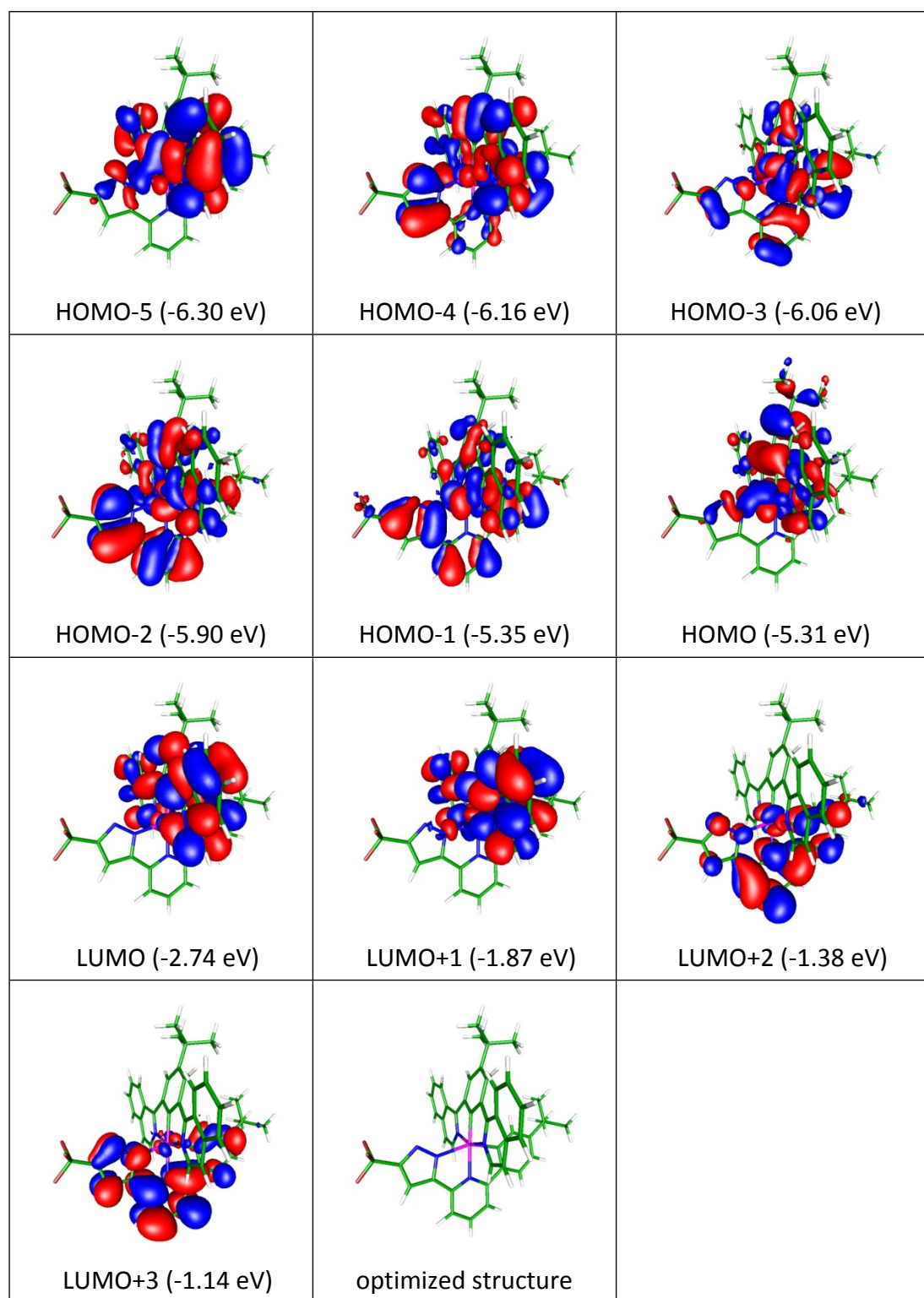


Figure S6. Frontier molecular orbitals pertinent to the optical transitions for complex **6**. For the clarity of viewing, the optimized structure with no involvement of frontier orbitals is shown at the last figure.